

## CHATTERING ANALYSIS OF AN ELECTRO-HYDRAULIC BACKSTEPPING VELOCITY CONTROLLER

Gérémino Ella Eny

Department of Physics, University of Sciences and Technologies of Masuku, GABON

Honorine Angue Mintsia Eya \*

Department of Mechanical Engineering, University of Sciences and Technologies of Masuku, GABON

E-mail: anguemintsa\_honorine@yahoo.fr

Rolland Michel Assoumou Nzue

Department of Mechanical Engineering, University of Sciences and Technologies of Masuku, GABON

Nzamba Senouveau

Department of Electrical engineering, University of Sciences and Technologies of Masuku, GABON

This paper focuses on the chattering analysis in a backstepping controller used to drive an electro-hydraulic servo system. The chattering phenomenon, well known in sliding mode control, strongly reduces operating performance while causing premature wear of the system. Four cases are studied to highlight the factors influencing the chattering in the backstepping control. In the first case, the effect of the unmodeled fast servo valve dynamics is analysed by comparing a reduced-order backstepping controller with a full-order controller. The second case analyses the sensitivity to the tuning gains of the backstepping controller. The third case emphasises the influence of the parameter of sign function approximation. The last case analyses the sensitivity of the parameter of the time derivative of the virtual controls. The simulation results in the Matlab/Simulink show that the chattering is mitigated by an appropriate gains tuning but above all an appropriate calculation of the derivatives of the virtual controls, particularly for high-order systems.

**Key words:** chattering analysis, backstepping controller, electro-hydraulic servo system, sensitivity analysis; fast unmodeled dynamics.

### 1. Introduction

Electro-hydraulic servo systems (EHSS) are those machines that handle large mechanical loads with precision, rapidity and robustness. Engineering applications use EHSS for automobile active suspension (Shaer *et al.* [1]), automobile power steering (Slavov *et al.* [2]), aerospace actuation (Slavov *et al.* [2]), robotic actuation (Binh *et al.* [3]), machine tools (Li *et al.* [4]), etc. The control laws that drive these huge industrial systems are mostly based on the linear control theory (Zhao *et al.* [5]) especially PID controllers [6]. However, the dynamics of the EHSS are strongly nonlinear (Kumawat *et al.* [7]) with parameter uncertainties (Merritt [8]). All these issues limit the performances of real-time EHSS operations and force researchers to turn to nonlinear control strategies.

In the literature, sliding mode control (SMC) and backstepping control are powerful approaches to manage nonlinearities. SMC consists of turning a full-order controlled system into a one-order controlled one by using a sliding mode surface or a desired trajectory (Slotine and Li [9]). Then, the first part of the control law is to reach the sliding mode surface and the second part with a discontinuous term is to keep the state variables inside it. For example, Sun *et al.* [10] use an adaptive reaching law in the SMC to quickly track the desired position of a hydraulic cylinder. Asymptotic convergence in the sliding surface is ensured using the

sign function as is shown in the work (Zheng and Su [11]). On the other side, backstepping control consists of dismantling the system into first-order subsystems which we define as virtual control. Then, the final control is deduced recursively using all the virtual controls (Krstic *et al.* [12]). Tri *et al.* [13] add an iterative learning scheme when constructing the virtual controls to overcome hydraulic parameter uncertainties. Experimental and numerical results show that these two nonlinear approaches give better performances than those obtained with PID controllers (Ghazali *et al.* [14]) and (Kaddissi *et al.* [15]).

However, the inconvenience of these previous approaches is the generation of high-frequency oscillations. This undesirable phenomenon known as chattering not only causes performance losses but also leads the system to premature wear. In the SMC, the chattering is mainly due to the discontinuous term or the sign function (Utkins and Hoon [16]). To reduce the chattering effect in a SMC, techniques like boundary layer (Has *et al.* [17]), sign function approximation (Ghani *et al.* [18]), observer disturbance (Long *et al.* [19]) and artificial intelligence (Feng *et al.* [20]) are proposed in the literature. If the chattering effect in the SMC is well documented in the literature, the chattering effect in backstepping control is very little studied. The works including chattering in EHSS backstepping control often identify the measurement noise (Won *et al.* [21]), SMC combination (Tran *et al.* [22]) or friction (Chen and Pen [23]) as the cause of chattering.

Literature lists several works regarding adjusting controller parameters to reduce chattering, particularly for sliding mode controllers. Failing to suppress chattering in their sliding mode controller, the describing function approach is used to adjust the controller gains to achieve the desired chattering frequency (Pilloni *et al.* [24], Castillo and Freidovich [25]). Frequency response analysis with the root locus tool is a method of adjusting the controller settings to stabilize chatter by damping the different captured frequencies (Beudaert *et al.* [26]). Because chattering is inherent to sliding mode controller, the authors Kuchwa-Dube and Pedro [27] propose a good measure of chattering criteria using Particle swarm optimization to tune the sliding mode controller gains. Combine adaptive tuning law with sliding mode controller allows the attenuation of chattering (Mobayen [28], Eltayeb *et al.* [29]). In the work of Huang *et al.* [30] and Chen *et al.* [23], the backstepping approach is used to reduce chattering effect while the present paper shows that chattering occurs in backstepping controllers. It should nevertheless be emphasised that several works in the literature show almost non-existent chattering and good performances in EHSS controlled with a backstepping control law (Binh *et al.* [3], Aela *et al.* [31], Wang *et al.* [32], Aela *et al.* [33], Zaare and Soltanpour [34]). In these closed-loop systems where chattering is minimized, the backstepping control law is generally combined with the adaptation law, neural networks approach, fuzzy control, optimisation and deep learning techniques.

The main contribution of this paper is to provide a deeper analysis of the chattering effect in a simple backstepping controller for an electro-hydraulic drive. This work is a continuation of the result of (Kaddissi *et al.* [15]) which highlights the relationship between the tuning gains and the chattering. However, in their work, this assertion is not demonstrated by simulations. Because literature reports that chattering can be the cause of the excitation of unmodeled fast dynamics (Fadil and Giri [35]), in this paper, chattering is firstly analysed by comparing the performances when a backstepping controller based on a full-order EHSS model with the backstepping controller based on the reduced EHSS model. Then, we investigate the influence of the tuning gains, the sigmoid function parameter and the parameter of the derivative of the virtual controls respectively using the Matlab/Simulink sensitivity analysis tool. These analyses are centered on the backstepping controller based on the full-order EHSS. The controller based on the reduced-order model is simply used on the EHSS to show the influence of the unmodeled dynamics. This controller is not studied in the other analysis cases. The scientific approach used in this paper to achieve our goal is presented in Fig.1.

The paper is structured as follows: The second section introduces the EHSS under study with two propositions of mathematical modelling. The third section shows the design of the the backstepping controller based on a full order modelling and the backstepping controller based on the reduced order modelling. In section 4, the simulation results are provided and discussed. Finally, the fifth section presents the conclusion.

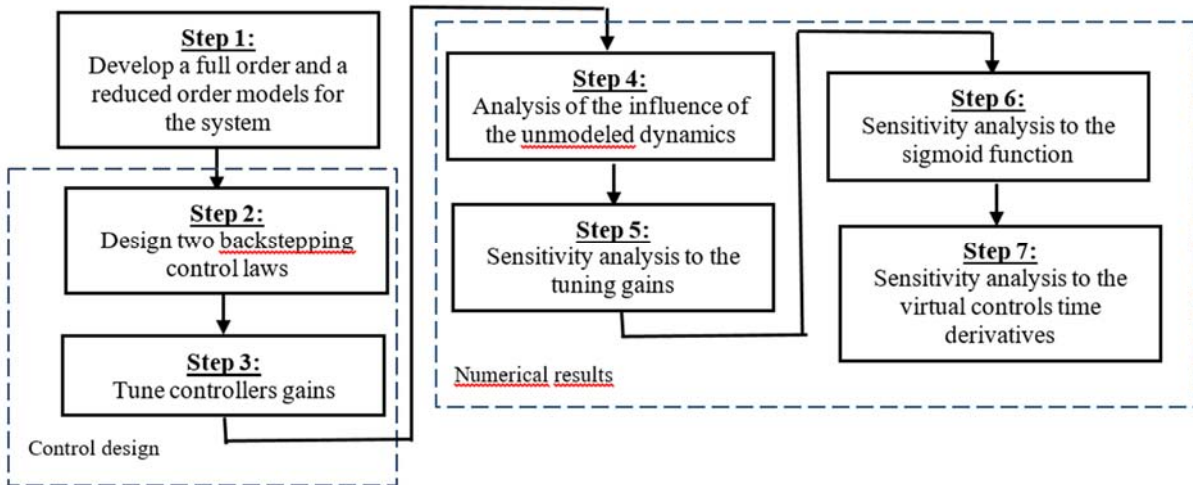


Fig.1. Research method of the paper.

## 2. System description and mathematical modellings

The electro-hydraulic servo system under study is illustrated in Fig.2. It is the same system used in our previous work (Angue-Mintsa *et al.* [36]). The hydraulic oil with a mass density  $\rho$  is pumped into the system using a pump. The servo valve supply pressure  $P_s$  is kept constant by the relief valve and the accumulator. The dynamics of the servo valve are approximated to the first order system with an amplifier gain  $K$  and a time constant  $\tau$ . The electrical input  $u(t)$  generates an oil passage area  $A_v(t)$  in the servo valve which has a discharge coefficient of  $c_d$ . When this passage is open, the hydraulic fluid passes through the servo valve to operate the motor which has a volumetric displacement of  $D_m$ . The total inertia, the total bulk modulus, the viscous damping coefficient, oil volume and leakage coefficient of the motor are respectively  $J$ ,  $\beta$ ,  $B_m$ ,  $V_m$ ,  $c_{sm}$ . A pressure difference  $P_L(t)$  is created between the motor lines due to the presence of the attached load. Then, the load is moved at the angular velocity  $\dot{\theta}(t)$  which is the output of the system and measured by a transducer.

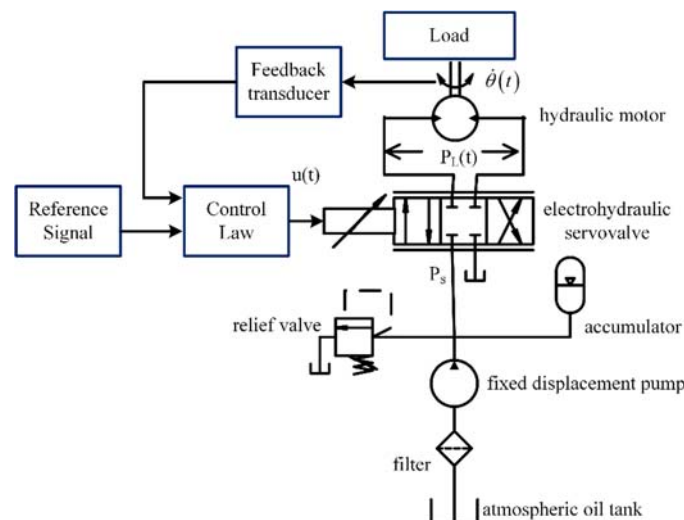


Fig.2. Electro-hydraulic servo system schematic.

## 2.1. Full-order state-space representation of the EHSS

The full order dynamics of the EHSS is defined using three variable states  $x_1(t) = \dot{\theta}(t)$ ,  $x_2(t) = P_L(t)$  and  $x_3(t) = A_v(t)$ . Thus, the third order nonlinear state space model Eq.(2.1) describes the equation of the load's motion, the equation of the continuity across the hydraulic motor and the dynamics of the electrohydraulic servo valve respectively

$$\begin{aligned}\dot{x}_1(t) &= \frac{D_m}{J} x_2(t) - \frac{B_m}{J} x_1(t), \\ \dot{x}_2(t) &= \frac{4\beta c_d}{V_m} \left( x_3(t) \frac{c_d}{\sqrt{\rho}} \sqrt{P_s - \text{sign}(x_3(t)) x_2(t)} - D_m x_1(t) - c_{sm} x_2(t) \right), \\ \dot{x}_3(t) &= \frac{K}{\tau} u(t) - \frac{l}{\tau} x_3(t), \\ y(t) &= x_1(t).\end{aligned}\tag{2.1}$$

## 2.2. Reduced-order state-space representation of the EHSS

Because the electro-hydraulic servo valve dynamics is very fast, we can neglect it as is done in the work (Ghani *et al.* [18]). Thus, the reduced order is obtained with the two order state space model Eq.(2.2). The index  $r$  is used to refer to reduced order.

$$\begin{aligned}\dot{x}_{1r}(t) &= \frac{d_m}{J} x_{2r}(t) - \frac{B_m}{J} x_{1r}(t), \\ \dot{x}_{2r}(t) &= \frac{4\beta c_d}{V_m} \left( K u_r(t) \frac{c_d}{\sqrt{\rho}} \sqrt{P_s - \text{sign}(u_r(t)) x_{2r}(t)} - d_m x_{1r}(t) - c_{sm} x_{2r}(t) \right), \\ y_r(t) &= x_{1r}(t).\end{aligned}\tag{2.2}$$

## 2.3. Sign function approximation

One can note that the two-state space models have two strong nonlinearities: the bilinear square root relationship and the discontinuous sign function. In order to satisfy the Lipschitz condition in this paper, we choose to approximate the sign function to the continuous function Eq.(2.3) proposed in the work of Shokouhi and Markazi [37] and illustrated in Fig.3. Here, the values on the abscissa correspond to the order of magnitude of the open sections of the servo valve .

$$\text{sign}(x(t)) \approx \frac{x(t)}{\sqrt{x^2(t) + \alpha}} = \text{sigm}(x(t))\tag{2.3}$$

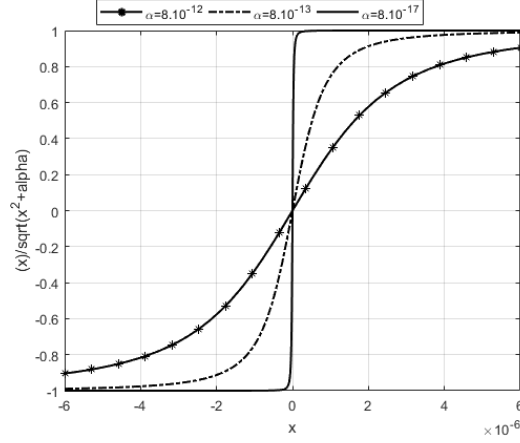


Fig.3. Sign function approximation.

### 3. Backstepping control design

In this section, we derive two backstepping controllers. The first one is derived using the full-order state space model as done in our previous works (Angue Mintsa *et al.* [36]). The second one is derived using the reduced-order state space model.

#### 3.1. Backstepping controller based on the full-order model

Readers are requested to find details of the development of this controller in our previous paper (Angue Mintsa *et al.* [36]). In this paper, we only present the two virtual controls ( $x_{2d}(t)$  and  $x_{3d}(t)$ ) and the deducing control signal  $u(t)$ . The variable  $x_{1d}(t)$  is the desired angular velocity given by the reference signal. The variable  $e_i(t)$  is the tracking error ( $e_i(t) = x_i(t) - x_{id}(t)$ ).

$$x_{2d}(t) = \frac{J}{d_m} \left( \frac{b_m}{J} x_{1d}(t) + \dot{x}_{1d} - k_{1f} e_1(t) \right), \quad (3.1)$$

$$x_{3d}(t) = \frac{v_m \sqrt{\rho}}{4\beta c_d \sqrt{P_s - \text{sigm}(x_3(t))} x_2(t)} \left[ -\frac{d_m}{J} e_1(t) + \right. \\ \left. + \frac{4\beta d_m}{v_m} x_1(t) + \frac{4\beta c_{sm}}{v_m} x_{2d}(t) + \dot{x}_{2d}(t) - k_{2f} e_2(t) \right], \quad (3.2)$$

$$u_f(t) = \frac{\tau}{K} \left( \frac{1}{\tau} x_{3df}(t) + \dot{x}_{3df}(t) + \right. \\ \left. - \frac{4\beta c_d}{v_m \sqrt{\rho}} e_{2f}(t) \sqrt{P_s - \text{sigm}(x_{3f}(t))} x_{2f}(t) - k_{3f} e_{3f}(t) \right). \quad (3.3)$$

With the gains  $k_{1f} > 0$ ,  $k_{2f} > 0$  and  $k_{3f} > 0$ ,

Figure 4 presents the architecture and the implementation of this control law in the Matlab/Simulink.

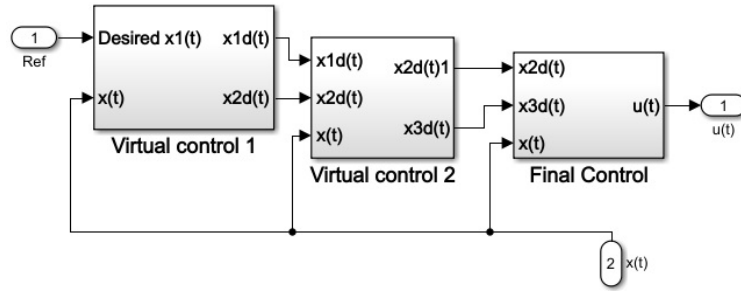


Fig.4. Block diagram of the full-order backstepping controller.

### 3.2. Backstepping controller based on the reduced-order model

To differentiate the reduced order variables from full-order variables, the  $r$  index is used. We can restart the backstepping procedure with the first candidate Lyapunov function as done in our previous work:

$$V_{1r}(t) = \frac{1}{2} e_{1r}^2(t). \quad (3.4)$$

Whose time derivatives gives

$$\dot{V}_{1r}(t) = e_{1r}(t) \left( \frac{d_m}{J} e_{2r}(t) + \frac{d_m}{J} x_{2dr}(t) - \frac{b_m}{J} e_{1r}(t) - \frac{b_m}{J} x_{1dr}(t) - \dot{x}_{1dr} \right). \quad (3.5)$$

Because the first subsystem is the same for the two models, the first virtual control is the same as that of the full-order backstepping controller  $x_{2dr}(t)$

$$x_{2dr}(t) = \frac{J}{d_m} \left( \frac{b_m}{J} x_{1dr}(t) + \dot{x}_{1dr} - k_{1f} e_{1r}(t) \right). \quad (3.6)$$

Where  $k_{1f} > 0$ , we deduce

$$\dot{V}_{1r}(t) = - \left( \frac{b_m}{J} + k_{1f} \right) e_{1r}^2(t) + \frac{d_m}{J} e_{2r}(t) e_{1r}(t). \quad (3.7)$$

For the last subsystem

$$\dot{x}_{2r}(t) = \frac{4\beta c_d}{V_m} \left( K u_r(t) \frac{c_d}{\sqrt{\rho}} \sqrt{P_s - \text{sigm}(u_r(t)) x_{2r}(t) - d_m x_{1r}(t) - c_{sm} x_{2r}(t)} \right),$$

the final candidate Lyapunov function is

$$V_{2r}(t) = \frac{1}{2} e_{1r}^2(t) + \frac{1}{2} e_{2r}^2(t). \quad (3.8)$$

Which leads to

$$\begin{aligned} \dot{V}_{2r}(t) = & -\left(\frac{b_m}{J} + k_{1r}\right)e_{1r}^2(t) + \\ & + e_{2r}(t) \left( \frac{d_m}{J} e_{1r}(t) + \frac{4K\beta c_d}{v_m \sqrt{\rho}} u_r(t) \sqrt{P_s - \text{sigm}(u_r(t))} x_{2r}(t) + \right. \\ & \left. - \frac{4\beta d_m}{v_m} x_{1r}(t) - \frac{4\beta c_{sm}}{v_m} x_{2r}(t) - \dot{x}_{2dr}(t) \right). \end{aligned} \quad (3.9)$$

By choosing

$$\begin{aligned} u_r(t) = & \frac{v_m \sqrt{\rho}}{4\beta K c_d \sqrt{P_s - \text{sigm}(u_r(t))} x_2(t)} \left( -\frac{d_m}{J} e_{1r}(t) + \right. \\ & \left. + \frac{4\beta d_m}{v_m} x_{1r}(t) + \frac{4\beta c_{sm}}{v_m} x_{2dr}(t) + \dot{x}_{2dr}(t) - k_{2r} e_{2r}(t) \right) \end{aligned} \quad (3.10)$$

where  $k_{2r} > 0$ , we obtain

$$\dot{V}_{2r}(t) = -\left(\frac{b_m}{J} + k_{1r}\right)e_{1r}^2(t) - \left(\frac{4\beta c_{sm}}{v_m} + k_{2r}\right)e_{2r}^2(t). \quad (3.11)$$

The final Lyapunov function is negative definite as expected. Figure 5 shows the architecture and the implementation of the reduced order backstepping controller in the Matlab/Simulink where the only virtual control is visible.

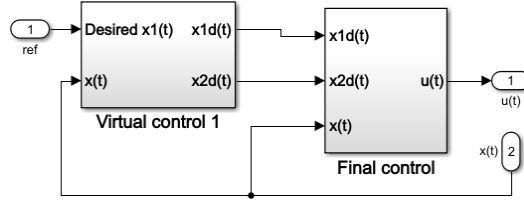


Fig.5. Block diagram of the reduced order backstepping controller.

### 3.3. Virtual controls time-derivative

The time-derivative of the virtual controls  $x_{id}(t)$  with  $i=1,2,3$  for the full-order backstepping controller and  $x_{idr}(t)$  with  $i=1,2$  for the reduced order backstepping controller are calculated using the filter of Eq.(3.12).  $s, X_i$  and  $X_{i\_deri}$  are the Laplace operator, the Laplace transform of the virtual control and its first derivative respectively.

$$X_{i\_deri}(s) = \frac{s}{d_i s + 1} X_i(s). \quad (3.12)$$

### 3.4. Tuning backstepping controllers' gains

Most gains adjustment of the backstepping controller are performed adaptively (Bihn *et al.* [3], Chen *et al.* [38]). Unlike the PID controller, the backstepping controller does not have a standardized method for adjusting gains. The authors Angue Mintsa *et al.* [39] fail to develop a heuristic method but show the prioritization of the gains. Optimization techniques are used to tune the backstepping controller gains. For example, Rodriguez-Abreo *et al.* [40] use the genetic algorithm for tuning a backstepping controller. In this paper, we use the analysis sensitivity and the response optimization tools in Matlab/Simulink to tune the gains of the two backstepping controllers.

We use a 2-step methodology to adjust the gains of the two controllers. Firstly, the sensitivity analysis of the minimum tracking error is carried out. This result gives an overview of the optimal values of each gain to be inserted in the initial conditions on the second step. Figure 6 shows the interface of the tool and the different criteria used for analysis.

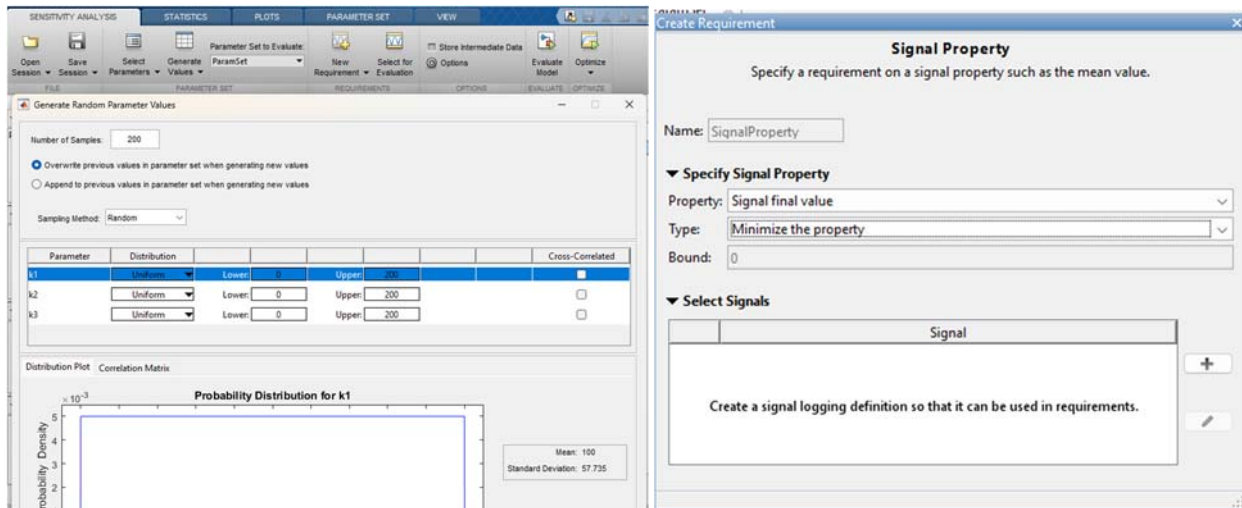


Fig.6. Interface of the Sensitivity Analysis tool in Matlab/ Simulink.

In the second step, we use the response optimization tool. The values of optimal gains values is used to refined the optimization process as shown in Fig.7. The requirement is set on the tracking on the reference signal by the output as shown in Fig.8. The optimal value of the gains are found after several iterations as shown in Fig.9.

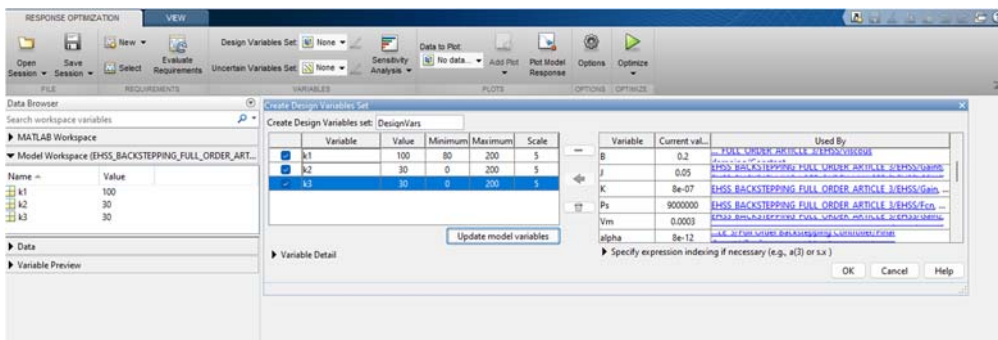


Fig.7. Interface of the Response Optimization tool in Matlab/ Simulink.

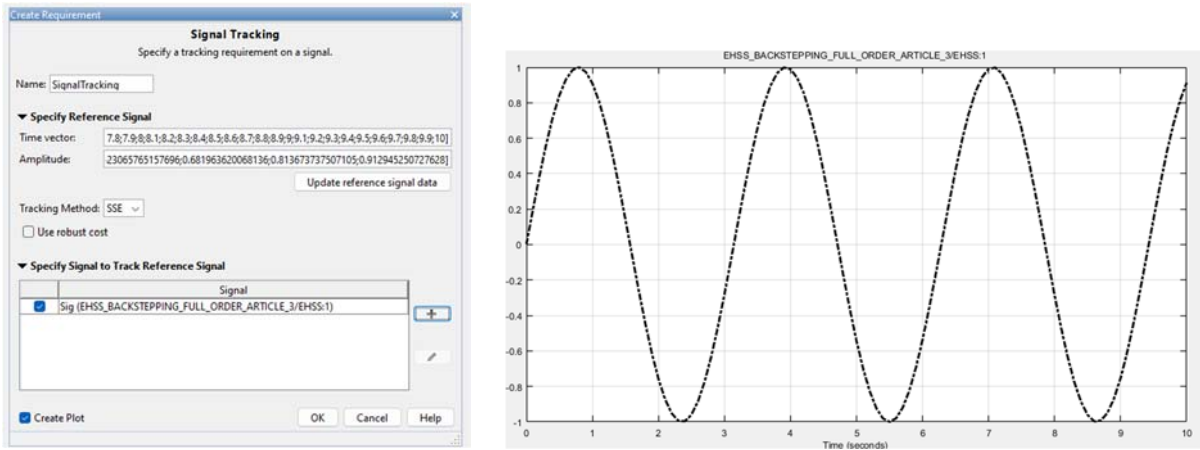


Fig.8. Requirement on the output for the Response Optimization.

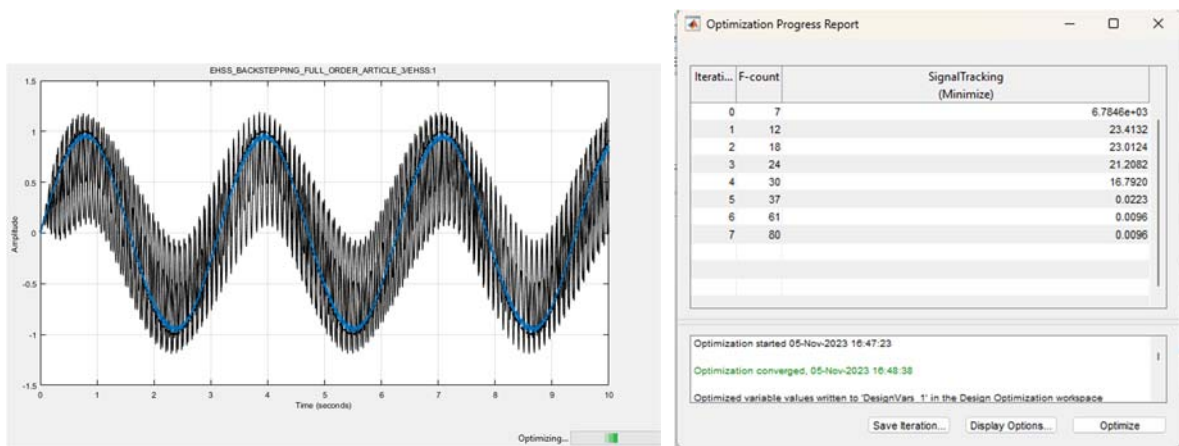


Fig.9. Iterative process for response optimization.

### 4. Numerical results

In this section, the results of the chattering analysis in the performances of the backstepping controller are presented. We recall that the study concerns the full order backstepping controller. The reduced order backstepping controller is only used to compare the influence of the unmodeled dynamics in the chattering. The simulation is run during 10 s and the sampling time is 10ms using the Matlab environment as shown in Fig.10. The reference signal is a sine wave of amplitude 1 rad/s with a frequency of 2rad/s. The numerical values are listed in the Tab.1.

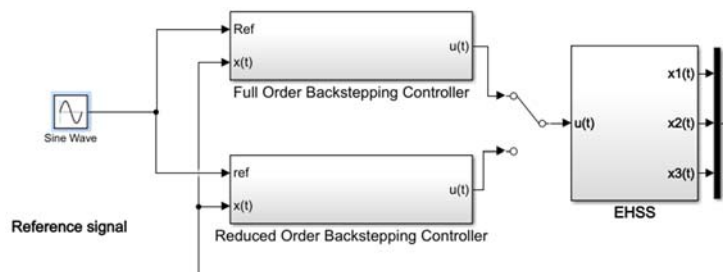


Fig.10 Architecture and implementation of the two controllers in the Matlab/Simulink.

Table 1. Numerical value.

Symbol	Definition	Value	units
<b>EHSS</b>			
$\tau$	time constant of the servo valve	0.01	s
$K$	amplifier gain of the servo valve	$8 \cdot 10^{-7}$	$m^2/mA$
$V_m$	fluid volume in the motor	$3 \cdot 10^{-4}$	$m^3$
$\beta$	oil bulk modulus	$8 \cdot 10^8$	Pa
$c_d$	discharge coefficient of the servo valve	0.61	
$P_s$	Supply pressure	$9 \cdot 10^6$	Pa
$c_{sm}$	Leakage coefficient	$9 \cdot 10^{-13}$	$m^5/(N.s)$
$d_m$	Volumetric displacement of the motor	$3 \cdot 10^{-6}$	$m^3/rad$
$\rho$	Fluid mass density	900	$Kg/m^3$
$J$	Motor inertia	0.05	$N.m.s^2$
$\alpha$	Sign function approximation coefficient	$8^{-12}$	
$B$	Motor damping coefficient	0.2	$N.m.s$
<b>Full order backstepping controller</b>			
$k_1$	Virtual control 1 gain	110	
$k_2$	Virtual control 2 gain	0	
$k_3$	Final control gain	95	
$d$	Analytic derivative coefficient for $x_{id}(t)$	$10^{-3}$	
<b>Reduced order backstepping controller</b>			
$k_{1r}$	gain of the virtual control 1	110	
$k_{2r}$	gain of the virtual control 2	95	
$\alpha$	Sign function approximation coefficient	$10^{-2}$	

#### 4.1. Case 1: Analysis of the influence of the unmodeled dynamics

This case shows the closed-loop performances obtained with both backstepping controllers. Their tuning parameters are almost the same (see Tab.1) and are established by the response optimization tool. The only difference is that one controller ignores the first-order dynamics of the servo valve. Figure 11 shows that both controllers perform well and appear to show the same results. However, the tracking errors comparison shown in Fig.12 shows that the backstepping controller based on the reduced order gives better results than the one based on the full order. The controller based on the full-order model exhibits overshoot, chattering and signal distortion while the controller based on the reduced order has light overshoots, no visible chattering and a smooth sinusoidal shape.

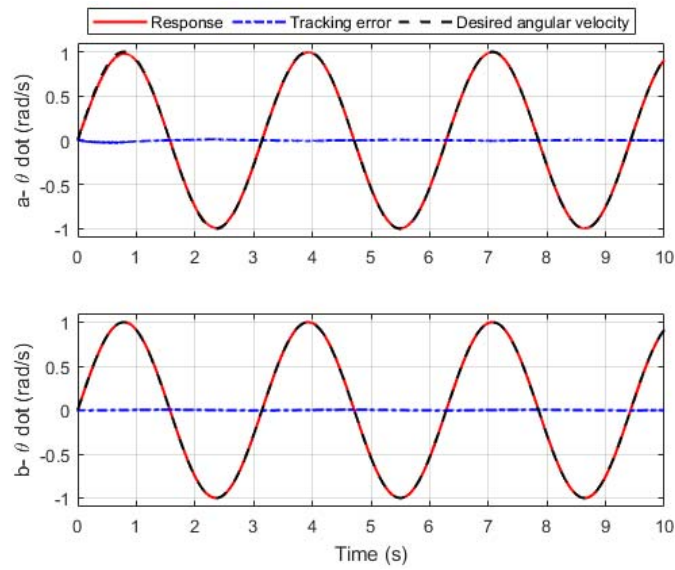


Fig.11. Closed-loop response with: a- the backstepping controller based on the full order b- the backstepping controller based on the reduced order.

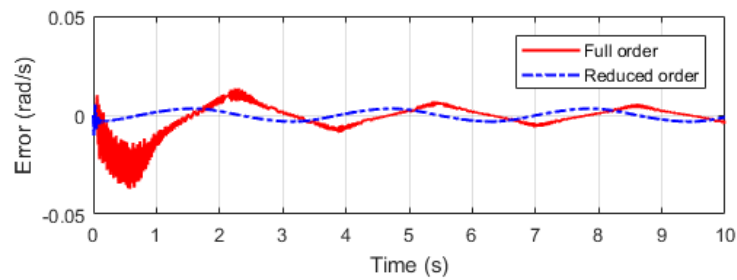


Fig.12. Tracking error of both backstepping controllers.

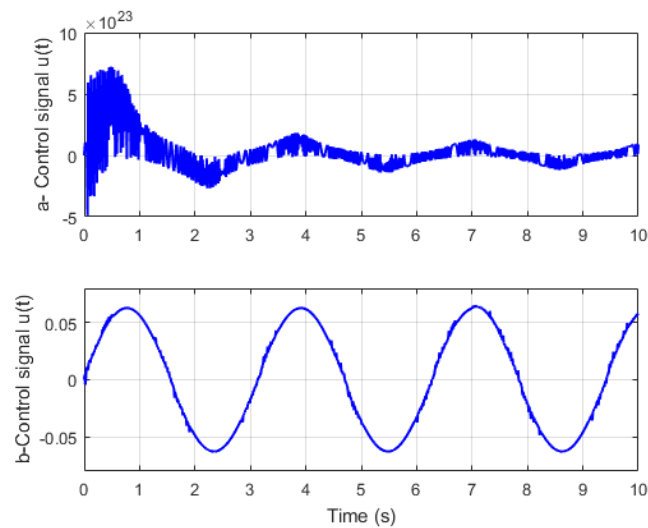


Fig.13. Control signal when using a- the backstepping controller based on the full order b- the backstepping controller based on the reduced order.

Figure 13 shows the control signal of both controllers. The backstepping controller based on the full order displays large control effort, significant chattering and signal distortion. The backstepping controller based on the reduced order shows a smooth control signal with a very small amplitude. Lee and Utkin [41] explain that chattering may be accentuated by the system’s unmodeled dynamics in the sliding mode controller. Based on the present results, we show that the backstepping controller based on unmodeled dynamics gives attenuation in chattering effects. Case study 4 may explain this phenomenon by analyzing the influence of the virtual control of the time-derivatives. Indeed, it is known that successive derivatives amplify the numerical noise. The backstepping controller based on the reduced order has the fewest virtual controls to derivate.

**4.2. Case 2: Control performances sensitivity analysis to the gains tuning**

The second case study concerns the influence of the backstepping controller gains adjustment. Figure 14 and Figure 15 show the sensitivity analysis of the control variance signal, the control final value and the tracking error to the three tuning gains. It is shown that the gain k1 has the most important influence on the minimization of the control variance while the gain k3 has the most important influence on the minimization of the control amplitude. From these figures, it is clear that when the value of k1 is above 100, the control variance, the control amplitude and the tracking error are minimized. The work of Angue Mintsu *et al.* [39] highlights the strong influence of the gain directly linked to the output. The influence of the gain k3 on the minimization of the control value can be explained again with the derivative of the virtual controls (case 4). The time derivative of the first virtual control was differentiated three times with the recursive backstepping process before being amplified by the final gain k3.

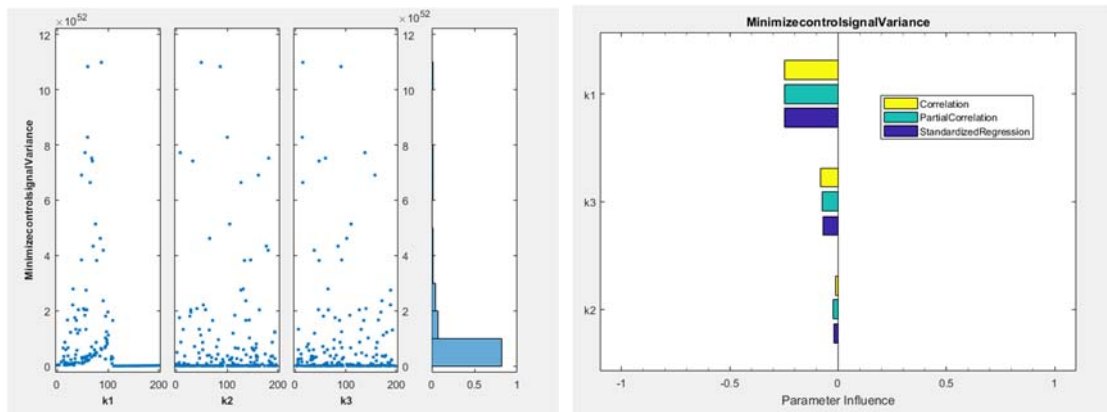


Fig.14. Sensitivity analysis of the minimum control variance to the tuning gains.

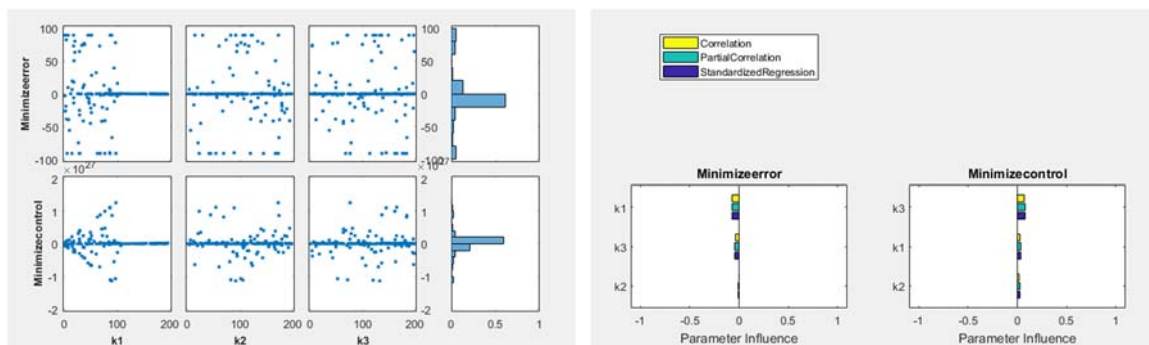


Fig.15. Sensitivity analysis of the minimum control final value and minimum tracking error to the tuning gains.

Figure 16 shows that reducing the gain  $k_1$  reduces the chattering in the control but can make the system response inaccurate. Figure 17 shows that increasing the gain  $k_3$  increases the chattering in the control while improving the tracking error. In both figures, one can note a dilemma between response accuracy and chattering reduction when adjusting the controller gains.

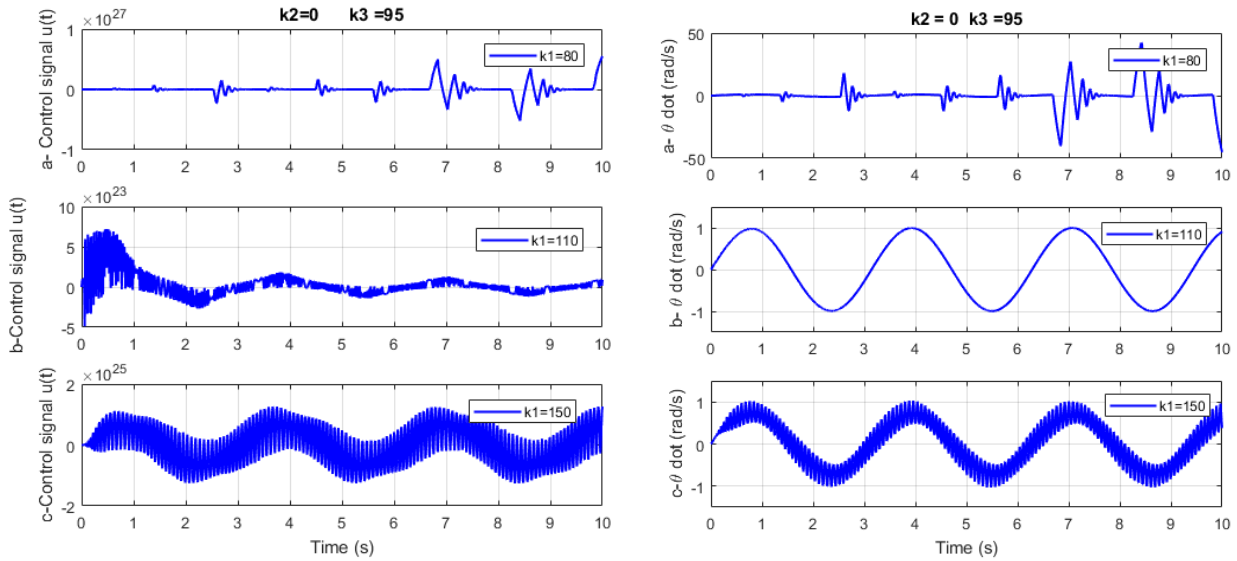


Fig.16. Control signal and system response with: a-  $k_1 = 80$  , b-  $k_1 = 110$  , c-  $k_3 = 150$  .

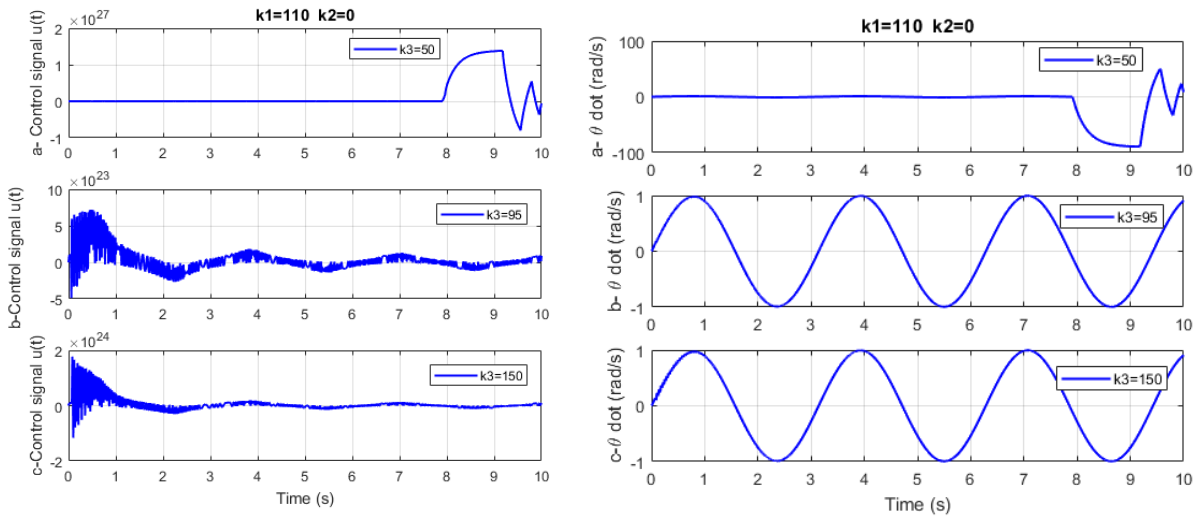


Fig.17. Control signal and system response with: a-  $k_3 = 50$  , b-  $k_3 = 95$  , c-  $k_3 = 150$  .

### 4.3. Case 3: Control performances sensitivity analysis to the sigmoid function

In this section, the sensitivity analysis of the chattering in the control signal to the sigmoid function parameter is studied. Indeed, it is well known that the discontinuous term on the sliding mode controller (SMC) leads to chattering (Lee and Utkin [41]). The SMC literature reveals that approximating the sign function mitigates chattering. In this article, the sigmoid function intervenes in the model and then in the backstepping control law. In the case of a backstepping controller applied to a nonlinear system where the dynamics is

discontinuous, we can think that the chattering occurs because of the switching term in the controller and that the approximation of the discontinuity by a continuous function may mitigate. However, Figure 18 shows that the chattering is not affected by the approximation of the sign function. Three different sigmoid parameters are selected based on different sign shapes shown in Fig.3. Figure 19 shows that the control and the system response are not significantly affected by the shape of the sigmoid function. Once again, we turn to the derivative of the virtual controls to explain the chattering in the backstepping controller (case 4).

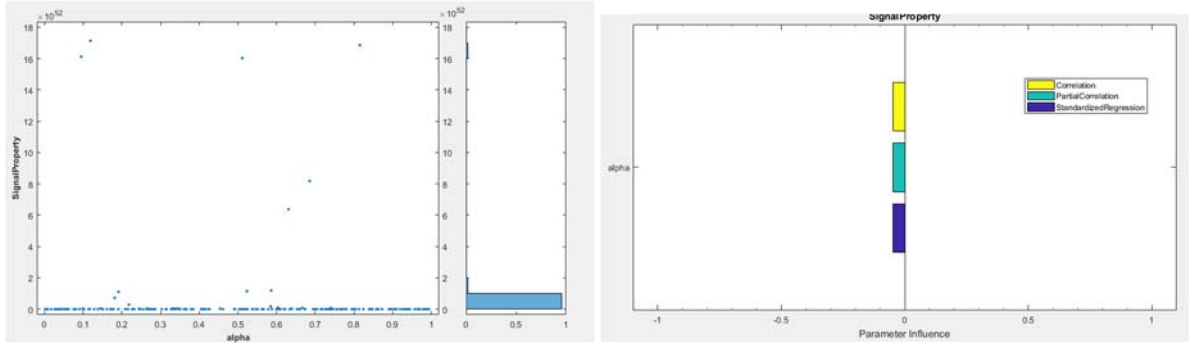


Fig.18. Sensitivity analysis of the minimum control variance to the parameter of the sigmoid function.

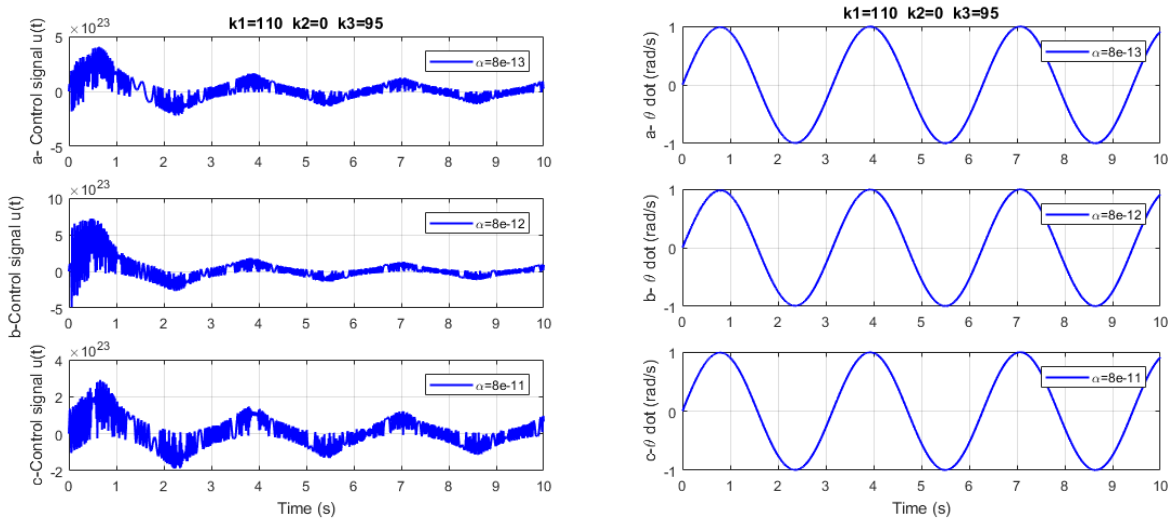


Fig.19. Control signal and system response with: a-  $k_3 = 80$  , b-  $k_3 = 110$  , c-  $k_3 = 150$  .

#### 4.4. Case 4: Control performances sensitivity analysis to the derivative of the virtual controls

This section presents the sets of simulation results regarding the influence of the derivative filters parameter in the chattering effects. These parameters  $d_1$ ,  $d_2$  and  $d_3$  are presented in section 3.3 of the article and their index indicates the virtual control to which they are assigned. Figure 20 shows that the parameter related to the derivative of the first virtual control has the largest influence when minimizing the control value and the control variance. Figure 20 clearly shows that the time derivative of the first virtual control affects the shape of the chattering in the control signal. A low value of the derivative filter parameter indicates a fast calculation of the derivative because the parameter  $d_i$  is the filter time constant. However, a rapid calculation of the time derivative leads to large non-uniform sustained oscillations while higher values of this parameter tighten and tend to standardize the chattering amplitude. We see that there is an optimal chattering ensuring good tracking error.

It can be noted that the results of case studies case 1, 2 and 4 are linked. We do not see a significant chattering in the backstepping controller based on the reduced model order because the recursive process differentiates the first virtual control twice while the one based on the full order differentiates this virtual control three times. In the scatterplot in section 4.2, the controller gain  $k_2$  is the least important to find a satisfactory tracking error because the second virtual control is directly included with  $k_3$  in the final controller.

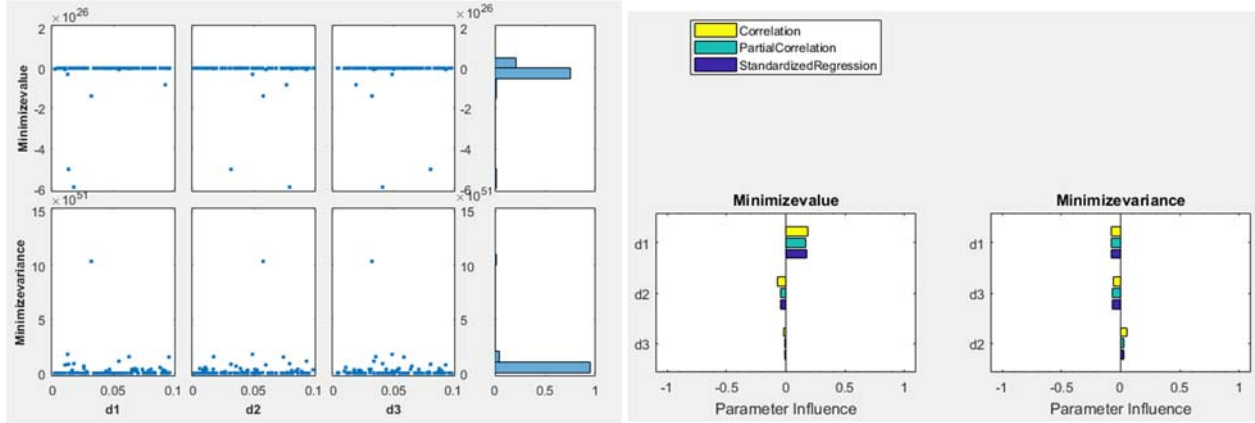


Fig.20. Sensitivity analysis of the control value and control variance to the parameters of the virtual controls derivative.

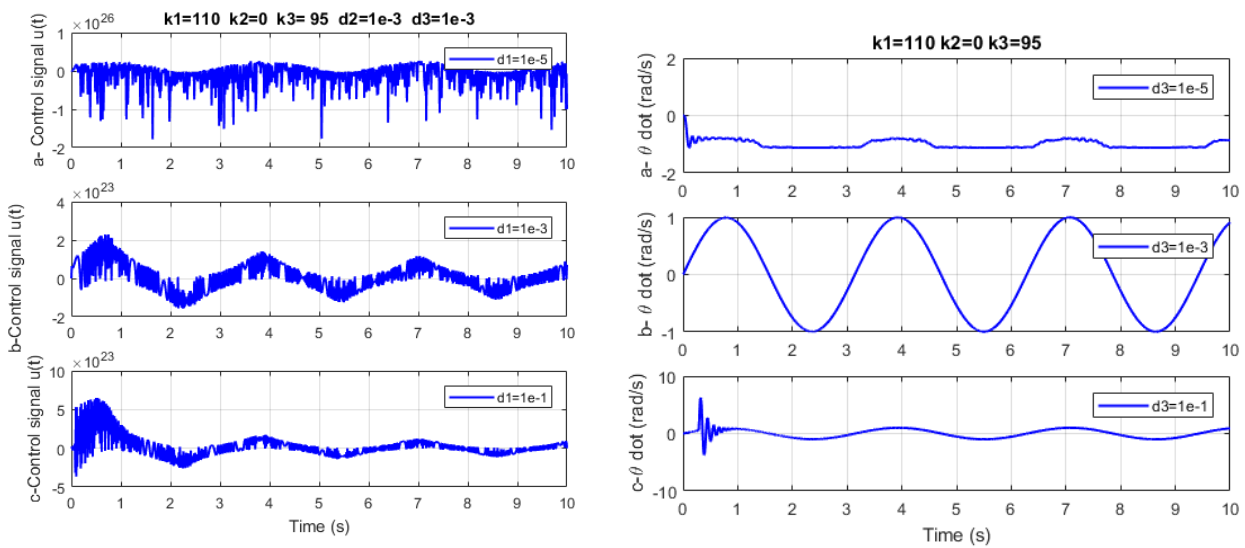


Fig.21. Control signal and system response with: a-  $d_3=10^{-5}$  b-  $d_3=10^{-3}$  c-  $d_3=10^{-1}$

### 5. Conclusion

This paper highlights the causes of chattering in the electrohydraulic velocity backstepping controller. Four possible causes were analysed in the control law: the unmodeled dynamics, the gains tuning, the shape of the sigmoid function and the derivative calculation of the virtual control. From this study, it appears that the main cause is the calculation of the time derivative of virtual controls amplified by the backstepping recursive process. Future works will investigate a backstepping controller law that is not sensitive to numerical noise by directly substituting the derivative expression into the virtual and final control equations.

## Nomenclature

- $A_v$  – oil passage area in the servovalve  
 $B_m$  – viscous damping coefficient of the hydraulic motor  
 $c_d$  – discharge coefficient of the electro-hydraulic servo valve  
 $c_{sm}$  – leakage coefficient  
 $d$  – analytic derivative coefficient  
 $D_m$  – volumetric displacement  
 $J$  – total inertia  
 $K$  – amplifier gain  
 $k_1$  – gain of the virtual control 1  
 $k_2$  – gain of the virtual control 2  
 $k_3$  – gain of the virtual control 3  
 $k_{1r}$  – gain of the virtual control 1 for the reduced order  
 $k_{2r}$  – gain of the virtual control 2 for the reduced order  
 $P_s$  – supply pressure  
 $t$  – time  
 $u(t)$  – input signal of the servo valve  
 $x_1(t)$  – angular velocity of the hydraulic actuator  
 $x_2(t)$  – pressure difference across the actuator  
 $x_3(t)$  – oil area passage in the servo valve  
 $y(t)$  – output of the system  
 $\alpha$  – sigmoid gain  
 $\beta$  – oil bulk modulus  
 $\dot{\theta}(t)$  – angular velocity of the hydraulic actuator  
 $\rho$  – oil mass density  
 $\tau$  – time constant of the servo valve

## References

- [1] Shaer B., Kenné J.-P., Kaddissi C. and Fallaha C. (2018): *A chattering-free fuzzy hybrid sliding mode control of an electrohydraulic active suspension.*– Transactions of the Institute of Measurement and Control, vol.40, No.1, pp.222-238.
- [2] Slavov T., Mitov A. and Krlev J. (2020): *Advanced embedded control of electrohydraulic power steering system.*– Cybernetics Information Technologies, vol.20, No.2, pp.105-121.
- [3] Binh N. T., Tung N. A., Nam D.P. and Quang N. H. (2019): *An adaptive backstepping trajectory tracking control of a tractor trailer wheeled mobile robot.*– International Journal of Control, Automation and Systems, vol.17, No.2, pp.465-473.
- [4] Li S., Yang Z., Tian H., Chen C., Zhu Y., Deng F. and Lu S. (2021): *Failure analysis for hydraulic system of heavy-duty machine tool with incomplete failure data.*– Applied Sciences, vol.11, No.3, p.1249.

- [5] Zhao X., Li L., Song J., Li C. and Gao X. (2016): *Linear control of switching valve in vehicle hydraulic control unit based on sensorless solenoid position estimation.*– IEEE Transactions on Industrial Electronics, vol.63, No.7, pp.4073-4085.
- [6] Kumawat A. K., Kumawat R., Rawat M. and Rout R. (2021): *Real time position control of electrohydraulic system using PID controller.*– Materials Today: Proceedings, vol.47, pp.2966-2969.
- [7] Merritt H. E. (1967): *Hydraulic Control Systems.*– John Wiley & Sons Inc.
- [8] Mintsu H. A., Venugopal R., Kenne J.-P. and Belleau C. (2011): *Feedback linearization-based position control of an electrohydraulic servo system with supply pressure uncertainty.*– IEEE Transactions on Control Systems Technology, vol.20, No.4, pp.1092-1099.
- [9] Slotine J.-J. E. and Li W. (1991): *Applied Nonlinear Control.*– Prentice hall Englewood Cliffs, NJ, vol.1.
- [10] Sun C., Dong X., Wang M. and Li J. (2022): *Sliding mode control of electro-hydraulic position servo system based on adaptive reaching law.*– Applied Sciences, vol.12, No.14, p.6897.
- [11] Zheng X. and Su X. (2021): *Sliding mode control of electro-hydraulic servo system based on optimization of quantum particle swarm algorithm.*– Machines, vol.9, No.11, p.283.
- [12] Krstic M., Kokotovic P.V. and Kanellakopoulos I. (1995): *Nonlinear and Adaptive Control Design.*– John Wiley & Sons, Inc.
- [13] Tri N. M., Nam D. N. C., Park H. G. and Ahn K. K. (2015): *Trajectory control of an electro hydraulic actuator using an iterative backstepping control scheme.*– Mechatronics, vol.29, pp.96-102.
- [14] Ghazali R., Sam Y. M., Rahmat M. and Hashim A. (2010): *Position tracking control of an electro-hydraulic servo system using sliding mode control.*– in 2010 IEEE student conference on research and development (SCOReD), pp.240-245: IEEE.
- [15] Kaddissi C., Kenne J. P. and Saad M. (2007): *Identification and real-time control of an electrohydraulic servo system based on nonlinear backstepping.*– IEEE/ASME Transactions on Mechatronics, vol.12, No.1, pp.12-22.
- [16] Utkin V. and Hoon L. (2006): *Chattering problem in sliding mode control systems.*– in International Workshop on Variable Structure Systems, 2006. VSS'06., pp.346-350.
- [17] Has Z., Rahmat M. F. A., Husain A. R. and Ahmad M. N. (2015): *Robust precision control for a class of electro-hydraulic actuator system based on disturbance observer.*– International Journal of Precision Engineering Manufacturing, vol.16, pp.1753-1760.
- [18] Ghani M. F., Ghazali R., Jaafar H. I., Soon C. C., Sam Y. M. and Has Z. (2022): *Improved third order pid sliding mode controller for electrohydraulic actuator tracking control.*– Journal of Robotics and Control, vol.3, No.2, pp.219-226.
- [19] Long L., Jian-Yong Y., Jian H., Da-Wei M. and Wen-Xiang D. (2015): *Tracking control for electro-hydraulic positioning servo system based on disturbance observer.*– Acta Armamentarii, vol.36, No.11, p.2053.
- [20] Feng H. Song Q, Ma S., Ma W., Yin C., Cao D. and Yu H. (2022): *A new adaptive sliding mode controller based on the RBF neural network for an electro-hydraulic servo system.*– ISA transactions, vol.129, pp.472-484.
- [21] Won D., Kim W., Shin D. and Chung C. C. (2014): *High-gain disturbance observer-based backstepping control with output tracking error constraint for electro-hydraulic systems.*– IEEE transactions on control systems technology, vol.23, No.2, pp.787-795.
- [22] Tran D. T., Ba D. X. and Ahn K. K. (2019): *Adaptive backstepping sliding mode control for equilibrium position tracking of an electrohydraulic elastic manipulator.*– IEEE Transactions on Industrial Electronics, vol.67, No.5, pp.3860-3869.
- [23] Chen L.-H. and Peng C.-C. (2017): *Extended backstepping sliding controller design for chattering attenuation and its application for servo motor control.*– Applied Sciences, vol.7, No.3, p.220.
- [24] Pilloni A., Pisano A. and Usai E. (2012): *Parameter tuning and chattering adjustment of super-twisting sliding mode control system for linear plants.*– in 12th International Workshop on Variable Structure Systems, pp.479-484.
- [25] Castillo I. and Freidovich L. B. (2020): *Describing-function-based analysis to tune parameters of chattering reducing approximations of Sliding Mode controllers.*– Control Engineering Practice, vol.95, p.104230, 2020/02/01/ .
- [26] Beudaert X., Franco O., Erkorkmaz K. and Zatarain M. (2020): *Feed drive control tuning considering machine dynamics and chatter stability.*– CIRP Annals, vol.69, No.1, pp.345-348.

- 
- [27] Kuchwa-Dube C. and Pedro J. O. (2022): *Chattering performance criteria for multi-objective optimisation gain tuning of sliding mode controllers.*– Control Engineering Practice, vol.127, p.105284.
- [28] Mobayen S. (2015): *An adaptive chattering-free PID sliding mode control based on dynamic sliding manifolds for a class of uncertain nonlinear systems.*– Nonlinear Dynamics, vol.82, No.1-2, pp.53-60.
- [29] Eltayeb A., Rahmat M. F. A., Basri M. A. M., Eltoum M. M. and El-Ferik S. (2020): *An improved design of an adaptive sliding mode controller for chattering attenuation and trajectory tracking of the quadcopter UAV.*– IEEE Access, vol.8, pp.205968-205979.

Received: October 4, 2023

Revised: January 17, 2024